HHS Public Access

Author manuscript

Inhal Toxicol. Author manuscript; available in PMC 2020 December 24.

Published in final edited form as:

Inhal Toxicol. 2019 ; 31(13-14): 446–456. doi:10.1080/08958378.2019.1705939.

Cultivation and aerosolization of *Stachybotrys chartarum* for modeling pulmonary inhalation exposure

Angela R. Lemons[a,*], **Tara L. Croston**[a], **W. Travis Goldsmith**[b], **Mark A. Barnes**[a], **Mukhtar A. Jaderson**[c], **Ju-Hyeong Park**[c], **Walter McKinney**[b], **Donald H. Beezhold**[d], **Brett J. Green**[a]

[a]Allergy and Clinical Immunology Branch, Health Effects Laboratory Division, National Institute for Occupational Safety and Health, Centers for Disease Control and Prevention, Morgantown, WV, USA

[b]Engineering and Control Technology Branch, Health Effects Laboratory Division, National Institute for Occupational Safety and Health, Centers for Disease Control and Prevention, Morgantown, WV, USA

[c]Field Studies Branch, Respiratory Health Division, National Institute for Occupational Safety and Health, Centers for Disease Control and Prevention, Morgantown, WV, USA

[d]Office of the Director, Health Effects Laboratory Division, National Institute for Occupational Safety and Health, Centers for Disease Control and Prevention, Morgantown, WV, USA

Abstract

Stachybotrys chartarum is a hydrophilic fungal species commonly found as a contaminant in water-damaged building materials. Although several studies have suggested that *S. chartarum* exposure elicits a variety of adverse health effects, the ability to characterize the pulmonary immune responses to exposure is limited by delivery methods that do not replicate environmental exposure. An acoustical generator system (AGS) was previously developed and utilized to aerosolize and deliver fungal spores to mice housed in a multi-animal nose-only exposure chamber. In this study, methods for cultivating, heat-inactivating, and aerosolizing two macrocyclic trichothecene-producing strains of *S. chartartum* using the AGS are described. In addition to conidia, acoustical generation of one strain of *S. chartarum* resulted in the aerosolization of fungal fragments (<2 μm aerodynamic diameter) derived from conidia, phialides and hyphae that initially comprised 50% of the total fungal particle count but was reduced to less than 10% over the duration of aerosolization. Acoustical generation of heat-inactivated *S. chartarum* did not result in a similar level of fragmentation. Delivery of dry, unextracted *S. chartarum* using these aerosolization methods resulted in pulmonary inflammation and immune cell infiltration in mice inhaling viable, but not heat-inactivated *S. chartarum*. These methods of *S. chartarum* growth and aerosolization allow for the delivery of fungal bioaerosols to rodents that may better simulate natural exposure within water-damaged indoor environments.

[*]corresponding author: Angela R. Lemons, Associate Service Fellow, Allergy and Clinical Immunology Branch, Health Effects Laboratory Division, National Institute for Occupational Safety and Health, Centers for Disease Control and Prevention, 1095 Willowdale Road, Morgantown, WV 26505, Tel: 1-304-285-6358.

Disclosure of interest

The authors declare no conflict of interest.

Keywords

fungi; fungal aerosolization; acoustical generator; inhalation exposure; fungal exposure; fungal fragments

Introduction

Personal exposure to mycotoxin producing hydrophilic fungi, such as *Stachybotrys chartarum*, has generated community and public health concern in the United States over the last two decades (CDC 1994; Montana et al. 1997; Etzel et al. 1998). *S. chartarum*, a darkly pigmented saprophytic fungus, requires a cellulose-rich nutrient medium and a high moisture content to support optimal growth (Andersson et al. 1997; Boutin-Forzano et al. 2004; Pestka et al. 2008). Based on these nutrient and growth requirements, *S. chartarum* is often identified as a building material contaminant in water-damaged indoor environments (Reponen et al. 2007; Madsen et al. 2016). In 1994, temporal associations between *S. chartarum* exposure and infant pulmonary hemosiderosis were reported by the Centers for Disease Control and Prevention (CDC 1994; Montana et al. 1997; Etzel et al. 1998), but these results were later revised due to limitations in the collection, analysis, and interpretation of the reported data (CDC 1997). *S. chartarum* has two chemotypes, with chemotype S producing macrocyclic trichothecenes and chemotype A producing namely atranones (Andersen et al. 2002; Andersen et al. 2003). These mycotoxins may contribute to the toxigenic health effects thought to be caused by *S. chartarum* exposure (Jarvis et al. 1998; Rao, Brain, et al. 2000). Rodent exposure to *S. chartarum* has been shown to elicit pulmonary inflammatory responses (Yike et al. 2003; Yike and Dearborn 2004; Yike et al. 2005; Ochiai et al. 2008; Lichtenstein et al. 2010), which is consistent with what has been observed following exposure in humans (Johanning et al. 1996; Hodgson et al. 1998). Exposure has also resulted specific IgE responses, suggesting that in addition to toxigenic health effects, *S. chartarum* may also contribute to allergic sensitization (Barnes et al. 2002; Chung et al. 2010).

Although preliminary studies have explored associations between *S. chartarum* exposure and adverse health effects, knowledge gaps regarding the pulmonary immunological mechanisms associated with the murine model are limited by *S. chartarum* delivery methods that do not replicate natural human exposure including: intranasal exposure (Nikulin et al. 1996), intratracheal instillation (Rao, Burge, et al. 2000; Rand et al. 2002; Yike et al. 2005; Ochiai et al. 2008), or liquid aerosol inhalation (Korpi et al. 2002) of spore suspensions or extracts. In order to better model the relationship between *S. chartarum* exposure and pulmonary responses, reproducible methods of *S. chartarum* cultivation and spore aerosolization are necessary to simulate natural exposure to dry, unextracted *S. chartarum* conidia.

The National Institute of Occupational Safety and Health has developed an acoustical generator system (AGS) for the delivery of fungal spores to mice housed in a nose-only exposure chamber (Buskirk et al. 2014). Aerosolization using this inhalation exposure system allows for real time measurements of particle size and mass concentration that is used to estimate the number of fungal particles deposited in the murine lung. To develop a

reproducible aerosolization method, our laboratory cultured *S. chartarum* on a cellulose substrate (rice) to replicate cellulose-containing building materials that act as a substrate within indoor environments. Heat inactivation of *S. chartarum* conidia was investigated for potential use in exposure studies as a biological particle control.

In this study, we describe methods of culture, heat-inactivation, and aerosolization of two *S. chartarum* chemotype S, or macrocyclic trichothecene-producing strains, IBT 9460 and IBT 7711, isolated from water-damaged buildings in Finland and Denmark, respectively (Andersen et al. 2002). To determine if these standardized methods can be implemented as a tool to model acute and subchronic exposure to fungal contaminants, repeated murine inhalation exposures were conducted to determine if dry *S. chartarum* aerosols delivered to the lung induced respiratory health effects.

Materials and methods

Fungal strains

Macrocyclic trichothecene-producing strains of *Stachybotrys chartarum*, IBT 9460 and *S. chartarum* IBT 7711, were used in this study. The 2 strains produced differing levels of macrocyclic trichothecene, with IBT 9460 (229.3 ±7.4 pmol per $1x10^6$ spores) producing over three times the amount of IBT 7711 (71.0 ±10.4 pmol per $1x10^6$ spores) as determined by extracting and analyzing macrocyclic trichothecenes from harvested spores using gas chromatography-tandem mass spectrometry as previously described (Saito et al. 2016). Using previously described methods, the internal transcribed spacer (ITS) region were sequenced using Sanger sequencing (Rittenour et al. 2014; Lemons et al. 2017) to confirm the identity of the 2 isolates used in this study. The ITS regions of the 2 strains were identical and were 100% homologous (100% coverage) with *S. chartarum* strain UAMH 7900 (accession AF081469) and *S. chartarum (chlorohalonata)* strain ATCC 9182 (accession AF081468) ITS 1 and 2 region sequences found in the National Center for Biotechnology Information (NCBI) database. While ITS region sequences for strains IBT 9460 and IBT 7711 were not found within the NCBI database, an 18S ribosomal RNA partial gene sequence for *S. chartarum* strain IBT 7711 (AF548096) overlapped with the first 210 base pairs of the ITS region sequence and was found to match with 100% homology.

Cultivation on rice

Each *S. chartarum* isolate was sub-cultured from glycerol stock sources and grown for 10-14 days at 26 °C (±2 °C) in standard unsealed Petri plates containing 15 mL of malt extract agar (MEA). *S. chartarum* particles including conidiogenous phialides, phialoconidia, and hyphae were liberated from the media in 2 mL of sterile distilled, deionized water using an inoculating loop. The suspension was diluted to a concentration of 2.5×10^5 spores/mL. White rice (Mahatma, Riviana Foods Inc., Houston, TX) was autoclaved in 250 mL flasks topped with aluminum foil (30 g/flask) with 10 mL water on a liquid cycle for 30 min at 121 °C. Rice was cooled and clumped rice was broken up prior to *S. chartarum* inoculation. Flasks containing sterile rice were inoculated with 5 mL of spore suspension (2.5×10^5 spores/mL) for each of the *S. chartarum* strains. Flasks topped with aluminum foil were

incubated at 26 °C (±2 °C) for 21-28 days at 60% (±5%) humidity. Flasks were shaken after 1 week of growth to prevent the rice from aggregating.

Heat inactivation of conidia

For generation of heat-inactivated particles, some 21-28 day *S. chartarum* cultures were incubated in a bead bath (Lab Armor, LLC, Cornelius, OR) at 80 °C for 2 hours with the foil cap remaining on the flasks. Viability was assessed for non-treated and heat-treated spores by plating 10^4 eluted spores on MEA and culturing at 26 °C (±2 °C) for 48-72 hours. The resulting fungal colony forming units (CFUs) were counted to determine spore viability. The percentage of viable spores within each suspension was determined by dividing the number of CFUs observed by the total number of spores plated.

Conidia protein extract analysis

Protein extracts were prepared by harvesting *S. chartarum* conidia in sterile water before and after heat-inactivation. Conidia were frozen at −80 °C prior to lyophilization overnight. Dried conidia were mixed with 300 mg 0.5 mm glass beads (soda lime; BioSpec Products, Inc., Bartlesville, OK) and processed in a bead mill homogenizer for 3 x 1 minute cycles at 4.5 m/s. Protein extract concentrations were determined using a Pierce BCA Protein Assay Kit (Thermo Fisher Scientific, Waltham, MA). Using a 4-20% polyacrylamide gel (Bio-Rad Laboratories, Inc., Hercules, CA), 20 μg of protein extract from viable and heat-inactivated conidia were separated using gel electrophoresis. The gel was stained with Imperial Protein Stain (Thermo Fisher Scientific) for 1 hour and destained overnight in distilled water. Images were captured using a Gel Doc EZ System (Bio-Rad Laboratories).

Aerosolization

After 21-28 days of growth, conidia-laden rice cultures were placed in a desiccator for 7-10 days prior to aerosolization. Viable and heat-inactivated *S. chartarum* conidia (IBT 9460 and IBT 7711) were aerosolized via the AGS as previously described (Buskirk et al. 2014). Briefly, HEPA-filtered air entered the modified PITT-3 generator where computer-controlled acoustical energy was used to vibrate a rubber membrane containing conidia-laden rice resulting in aerosolization (Figure 1). Sample ports were placed within the exposure chamber to measure particle size and concentration, as well as to collect samples for electron microscopy and quantification of verrucarol.

Aerodynamic particle size measurements

Particle size distributions and count concentrations were measured in real-time using an aerodynamic particle sizer (APS; TSI Inc., Shoreview, MN) while real-time mass concentrations were determined with a calibrated DataRAM 4 light scattering device (ThermoElectron Co., Franklin, MA). The DataRAM 4 was calibrated daily by comparing its 1 hour average concentration to the actual average concentration measurements determined by gravimetric filter readings (0.45 μm pore size 37 mm diameter PTFE filters with 0.20 mL/min sample flow). To compare the size distributions observed between each strain and treatment, the raw counts obtained following aerosolization were normalized

based on the particle count concentration observed in the chamber when the measurements were recorded.

Verrucarol quantification from polycarbonate filters

Fungal material was aerosolized using the AGS and collected onto 25 mm 0.2 μm pore size Whatman polycarbonate filters (Whatman/GE Healthcare, Chicago IL) at a flow rate of 0.2 L/min until approximately 2 x 10^6 spores were deposited on the filter. Total spore counts were determined using the APS. The filters were placed in a glass tube and one milliliter of extraction solution (a combination of 99% acetonitrile and 1% acetic acid by volume) was added. The tube was incubated overnight and then sonicated for an hour with 1 minute of vortexing every 20 minutes. The tube was centrifuged for 3 minutes at 2000 x g and 700 μL of the supernatant was transferred to an injection vial that was dried under gentle nitrogen stream. Once dried, 200 μL of 0.2 M methanolic NaOH was added to the vial, which remained under the chemical hood overnight to hydrolyze macrocyclic trichothecene to verrucarol. On the third day, the contents of the vial were dried by gentle nitrogen stream and then reconstituted by 200 μL of injection solution (a combination of 69% water, 30% methanol, and 1% acetic acid by volume) and vortexed for 30 seconds. Finally, 10 μL of the sample extract was injected into a Ultra Performance Liquid Chromatograph coupled to a tandem Mass Spectrometer (UPLC/MSMS, Acquity H Class UPLC and Acquity Xevo TqD Quadrupole Tandem Mass-Spectrometer, Waters, Massachusetts, USA). Verrucarol (molecular weight 266.2 g/mol; retention time = 4.9 minute) was identified and quantified with two transitions from a precursor ion (267.1 dalton, [M+H]+) to product ions with molecular weights of 249.1 and 231.1 dalton at collision energy of 6 and 12 kV (at cone voltage of 52kV), respectively.

Field emission scanning electron microscopy

Aerosolized fungal particles were collected on 25 mm 0.2 μm pore size Whatman polycarbonate filters (Whatman/GE Healthcare, Chicago IL) at a flow rate of 1 L/min for approximately 5 seconds. The filter was attached with double-stick carbon tape to an aluminum mount and sputter coated with gold/palladium. Images were then collected on a Hitachi S-4800 (Tokyo, Japan) field emission scanning electron microscope.

Animals and inhalation exposures

Female B6C3F1/N mice aged 5-6 weeks were obtained from Taconic Biosciences, Inc. (Germantown, NY) and were maintained in the AAALAC International accredited animal facility located at the National Institute for Occupational Safety and Health (NIOSH, Morgantown WV). Mice were provided NTP2000 diet (Harlan Laboratories, Madison, WI) and tap water *ad libitum*. All procedures were conducted under an approved NIOSH Animal Care and Use Committee protocol. After a one-week facility acclimation and one week of acclimation to the exposure pods, mice were exposed twice a week for a total of 4 weeks (8 exposures) to aerosolized *Stachybotrys chartarum* until 1 x 10^4 conidia were estimated to be deposited in the lung as previously described (Buskirk et al. 2014; Croston et al. 2016). Exposure groups included HEPA-filtered air-only (n=30), *S. chartarum* IBT 9460 viable (n=15) and heat-inactivated (n=15), and *S. chartarum* IBT 7711 viable (n=15) and heat-inactivated (n=15). Measurements of temperature, humidity and gravimetric mass

concentration recorded during the 8 exposures (Table 1) were consistent among each of the strains. Twenty-four hours following the final exposure, mice were euthanized via intraperitoneal injection of 200 mg/kg sodium pentobarbital solution (Fatal-Plus, Vortech Pharmaceuticals, LTD., Dearborn, MI) followed by exsanguination via cardiac puncture. Bronchoaveolar lavage fluid (3 mL) and lung tissue were collected following euthanasia.

Flow cytometry analysis

Bronchoalveolar lavage (BAL) with 1 mL phosphate buffered saline (pH 7.2) was performed 3 times following euthanasia. Cells collected in the BAL (n=7 per exposure group) were enumerated using a Cellometer Vision CBA (Nexcelom Bioscience, Lawrence, MA) and prepared for flow cytometric analysis as previously described (Nayak et al. 2018). Cells were incubated with Fc Block (CD16/CD32) (BD Biosciences, San Jose, CA, USA) and rat serum (Sigma-Aldrich, St Louis, MO, USA) prior to staining with the following BD Biosciences fluorochrome-conjugated antibodies: APC Hamster Anti-Mouse CD3e clone 145-2C11, Alexa Fluor 700 Rat Anti-Mouse CD4 clone RM4-5, APC-H7 Rat Anti-Mouse CD8 clone 53-6.7, BV786 Rat Anti-Mouse CD19 clone 1D3. Stained cells were evaluated using a BD LSR II (BD Biosciences) and the resulting data was analyzed using FlowJo (FlowJo LLC, Ashland, OR).

Histopathologic analysis of lung tissues

Murine lungs were harvested and the left lung lobes (n=3 per exposure group) were tied off, perfused with formalin, and then paraffin embedded and sectioned at 5 microns as previously described (Nayak et al. 2018). Sections were hematoxylin and eosin (H&E) stained for histopathology evaluation. Representative photomicrographs were captured using Olympus AX-70 (Olympus Corporation, Central Valley, PA, USA) microscope with DP73 (Olympus) digital camera. Images were captured using a 20x objective.

Statistical analysis

Verrucarol quantification was statistically evaluated using a two-way analysis of variance (ANOVA) followed by a Sidak's multiple comparison test to determine the source of variation. Cell populations evaluated by flow cytometry were analyzed by one-way ANOVA followed by a Dunnett's multiple comparison test to compare each test group to the air-only control. A p value less than or equal to 0.01 was considered statistically significant. All analyses were performed using GraphPad Prism v. 7 (GraphPad Software Inc., San Diego, CA)

Results

Cultivation and heat-inactivation of S. chartarum

Cultivation of *S. chartarum* on rice resulted in the growth and sporulation of fungi on a cellulose-based substrate that could be easily disturbed to release fungal spores and fragments. The cultures were shaken mid-incubation to allow for individual rice grains to be almost entirely coated in *S. chartarum* (Figure 2). To reduce *S. chartarum* conidia viability, some flasks were heat-treated at 80 °C. The heat-treatment resulted in 100% reduction in spore viability in both *S. chartarum* strains tested (Table 2). Although the viability of the

conidia was reduced, the morphology of the spores remained intact (Figure 3). Analysis of the protein profiles of extracted conidia demonstrated a loss or reduction in most proteins larger than 15 kD (Figure 4). Endotoxin was detected on both conidia-laden and uninoculated rice at levels less than 0.1 EU/ mg rice grain for all samples tested.

Aerosolization of S. chartarum conidia

The viable and heat-inactivated cultures were aerosolized using the AGS and the aerodynamic particle size distribution of the bioaerosols produced ranged from <0.5 μm to 8 μm and peaked between 3 and 5 μm (Figures 5 & 6). The APS data as well as SEM analysis suggested that the aerosol consisted primarily of single spores but also included clusters of conidia as well as fragments derived from fungal particulate. The two strains behaved similarly during aerosolization; however, the aerosol derived from the higher toxin-producing strain (IBT 9460) was comprised of more small fragments (<0.5-2 μm) during early aerosolization as shown by the size distribution of the aerosol particulate (Figure 5). While fragments were observed in the >2 μm fraction of strain IBT 9460, the fungal material aerosolized within the 3-5 μm range of both strains was derived from primarily single spores. The fragmentation that occurred with viable strain IBT 9460 did not appear during aerosolization of its heat-inactivated counterpart (Figures 6, Table 3). Aerosolization of viable and heat-inactivated *S. chartarum* IBT 7711 resulted in particle distributions that were nearly identical (Figure 5, Table 3).

Analysis of the two *S. chartarum* aerosols revealed that at early time points (<20 min), 50% of the total particle counts from strain IBT 9460 were derived from fragments with an aerodynamic diameter measuring ≤2 μm compared to IBT 7711 fragments comprising less than 5% of the total fungal aerosol count (Table 3). These fragments appeared as early as 5 minutes in the aerosolization time course and began to taper off by 20 minutes (Figure 6). At this point, the fragmentation of conidia and hyphae from IBT 9460 was reduced to approximately 10% of the total fungal particle counts (Table 3) and the size distribution looked similar to that of IBT 7711 (Figure 5). Interestingly, less than 10% of the fungal particle counts derived from the heat-treated IBT 9460 fell in the ≤2 μm aerodynamic diameter size fraction. The source of the fragments observed in *S. chartarum* IBT 9460 were microscopically determined to be derived from the organism and not from the rice substrate itself. Acoustical generation of un-inoculated rice revealed that no fragments were aerosolized into the chamber. Based on the surface architecture of the small fragments observed through scanning electron microscopy, it is hypothesized that the fragments were derived from *S. chartarum* spores, phialides and hyphae (Figure 7).

Verrucarol, a hydrolysis product of macrocyclic trichothecene, was detected on filters sampled from within the exposure chamber following the aerosolization of *S. chartarum* (Figure 8). The viable and heat-treated aerosols demonstrated similar levels of verrucarol with no statistically significant difference observed. Strain IBT 9460 produced approximately 4 times the amount of IBT 7711. This difference was determined to be statistically significant ($p < 0.01$). Endotoxin levels measured on all test filters were 0.03 EU or less per filter (LOD=0.023 EU/filter). The levels following *S. chartarum* aerosolization were similar to those measured in air-only and rice-only control filters.

Murine Inhalation Exposures

Following inhalation of *S. chartartum* aerosols (estimated lung deposition of 1 x 10^4 spores), airway inflammation was observed after exposure to both strains of viable *S. chartarum* (Figure 9). The extent of inflammation was more pronounced in strain IBT 9460 compared to IBT 7711. In addition, analysis of lymphocyte populations in the bronchoalveolar lavage fluid revealed significant increases in B and T cells following exposure to viable *S. chartarum* IBT 9460 (Figure 10). Exposure to IBT 7711 resulted in increased CD8+ T cell populations, but not CD4+ T cell or B cell populations. Lung histology following exposure to heat-inactivated *S. chartarum* was similar to air-only controls (Figure 9) and no significant changes in lymphocyte populations were observed (Figure 10).

Discussion

Methods for aerosolizing fungi that better mimic natural exposures in contaminated environments are required to gain a better understanding of the health effects that result following exposure. This study describes a method of *S. chartarum* cultivation on rice, a solid cellulose substrate that is similar to building materials that are often susceptible to fungal growth. Cultivation on rice allows for spores and other fungal particulates to be easily disturbed and aerosolized without the need for high speed air, which has been used in previous inhalation models using building materials as the culture substrate (Brasel et al. 2005; Cho et al. 2005; Mensah-Attipoe et al. 2016). Aerosolization using the AGS system described here resulted in a bio-aerosol comprised of only *S. chartarum*-derived particles, as fragments of substrate shown to be confounding variables in studies utilizing building materials were not observed.

In addition to cultivation on rice, this study describes a method of heat-inactivation for the development of a non-viable *S. chartarum* aerosol. Previous studies have demonstrated that spore viability and in vivo germination influence the pulmonary immune response (Templeton et al. 2011; Nayak et al. 2018). As natural exposures to fungi include both viable and non-viable fungal particles, it is important to understand the contribution of each following inhalation exposure. The developed method of *S. chartarum* cultivation and heat-inactivation resulted in reproducible dry aerosol suspensions consisting primarily of single conidia that can be feasibly delivered to rodents for nose-only murine inhalation studies.

Aerosolization of *S. chartarum* IBT 9460 resulted in the production of fragments ranging in size from <0.5 μm to 2 μm aerodynamic diameter that made up 50% of the total fungal particle counts. This fragmentation was present at early aerosolization time points (within the first 20 minutes) and tapered off to 10% over time. The heat-treated cultures did not produce these small fragments for reasons that remain unclear. As *S. chartarum* spores are on average approximately 4.6 μm in aerodynamic diameter (Sorenson et al. 1987; Reponen 1995), it was presumed that the particles aerosolized within the <2 μm aerodynamic diameter size range were fragments derived from both spores and hyphae and did not consist of intact spores, which was confirmed by scanning electron microscopy. Similar to the *S. chartarum* fragments released in this study, the release of fungal particles from moldy building materials has been shown to result in the aerosolization of submicron fragments (Madsen et al. 2016; Mensah-Attipoe et al. 2016). While the fungal fragments acoustically

generated in the present study accounted for up to half of the fungal particle count concentration, fungal fragments derived from a non-toxin producing isolate of *S. chartarum* were released using high air flow at a concentration over 500 times higher than that of spores (Cho et al. 2005). Using a computer-based model, the deposition of these fungal fragments in the human respiratory tract was predicted to be over 200 fold higher than spores (Cho et al. 2005). Within indoor environments, fungal fragments have been shown to contribute to the overall fungal biomass (Reponen et al. 2007; Adhikari et al. 2013). In a field study, submicron fractions collected with a cyclone air sampler revealed 1,3 β-*D*-glucan concentrations that were similar or higher than that of the spore fractions (Reponen et al. 2007), indicating that their contribution to personal exposure may be substantial.

This study also demonstrated that both viable and non-viable fungi contain trichothecene mycotoxins, which have been shown to cause negative health effects (Islam et al. 2006; Carey et al. 2012). Detection of verrucarol on the filters suggests that murine exposure to aerosolized *S. chartarum* could result in exposure to the mycotoxins and secondary metabolites produced by the organism. Although trichothecenes were not directly measured in the small fragment fraction in this study, trichothecene mycotoxins have been shown to be associated with submicron fragments as well as spores derived from *S. chartarum* (Brasel et al. 2005), suggesting that the smaller fragments aerosolized following acoustical generation are biologically relevant in terms of overall fungal exposure. In addition, enzyme-linked immunosorbent assay analyses of fungal bioaerosols derived from *Aspergillus* and *Penicillium* species (Górny et al. 2002) and immunodetection of *Aspergillus versicolor* fragments by FESEM (Afanou et al. 2015) demonstrated that both fungal fragments and spores contain common antigens, further emphasizing the potential biological importance of exposure to these submicron fungal particles.

This study describes the feasibility of cultivating and aerosolizing *S. chartarum* for application in animal inhalation exposure studies that better simulate human exposure in contaminated indoor environments. While the majority of the bioaerosol was made up of homogenous single spores, we demonstrated that one of the *S. chartarum* strains produced significant amounts of respirable fungal fragments within the first 20 minutes of aerosolization. These fragments accounted for up to half of the overall fungal count concentration observed following aerosolization by acoustical generation. Additionally, mycotoxins and other secondary metabolites were also detectable in the aerosol. Murine inhalation exposure to viable, but not heat-inactivated, *S. chartarum* bioaerosol resulted in airway inflammation as well as T and B cell infiltration. The extent of immune cell infiltration and inflammation was greater following exposure to strain IBT 9460, which produced more trichothecene and more respirable fungal fragments upon aerosolization. Given that a similar amount of trichothecene was detected in heat-inactivated and viable IBT 9460 filters following aerosolization, it can be hypothesized that the increase in respirable fungal fragments produced during IBT 9460 aerosolization may be influencing the pulmonary immune responses following exposure. This hypothesis is supported by previous studies showing higher concentrations of fungal fragments in the homes of asthmatic children compared to homes of non-asthmatic children (Seo et al. 2014). These fragments and associated metabolites represent a contribution to the overall exposure that may influence adverse health effects following the inhalation of *S. chartarum* bioaerosols.

Acknowledgements

The authors would like to thank Jared Cumpston, Howard Leonard, James B. Cumpston, Amy Cumpston and Michelle Donlin for their assistance in the aerosolization of the test articles. The authors would also like to thank the NIOSH histopathology core for processing and staining lung sections for analysis, Diane Schwegler-Berry and Sherri Friend for field emission scanning electron microscopy analyses, and Yeonmi Park for endotoxin analyses. This study was supported in part by an interagency agreement between NIOSH and NIEHS (AES12007001-1-0-6) as a collaborative National Toxicology Program research activity. The findings and conclusions in this report are those of the authors and do not necessarily represent the official position of the National Institute for Occupational Safety and Health, Centers for Disease Control and Prevention.

References

Adhikari A, Reponen T, Rylander R. 2013 Airborne fungal cell fragments in homes in relation to total fungal biomass. Indoor Air. 23(2):142–147. [PubMed: 22804753]

Afanou KA, Straumfors A, Skogstad A, Nayak AP, Skaar I, Hjeljord L, Tronsmo A, Eduard W, Green BJ. 2015 Indirect immunodetection of fungal fragments by field emission scanning electron microscopy. Applied and Environmental Microbiology. 81(17):5794–5803. [PubMed: 26092450]

Andersen B, Nielsen KF, Jarvis BB. 2002 Characterization of *Stachybotrys* from water-damaged buildings based on morphology, growth, and metabolite production. Mycologia. 94(3):392–403. [PubMed: 21156510]

Andersen B, Nielsen KF, Thrane U, Szaro T, Taylor JW, Jarvis BB. 2003 Molecular and phenotypic descriptions of *Stachybotrys chlorohalonata* sp. nov. and two chemotypes of *Stachybotrys chartarum* found in water-damaged buildings. Mycologia. 95(6):1227–1238. [PubMed: 21149024]

Andersson MA, Nikulin M, Koljalg U, Andersson MC, Rainey F, Reijula K, Hintikka EL, Salkinoja-Salonen M. 1997 Bacteria, molds, and toxins in water-damaged building materials. Appl Environ Microbiol. 63(2):387–393. [PubMed: 9023919]

Barnes C, Buckley S, Pacheco F, Portnoy J. 2002 IgE-reactive proteins from *Stachybotrys chartarum*. Ann Allergy Asthma Immunol. 89(1):29–33. [PubMed: 12141716]

Boutin-Forzano S, Charpin-Kadouch C, Chabbi S, Bennedjai N, Dumon H, Charpin D. 2004 Wall relative humidity: a simple and reliable index for predicting *Stachybotrys chartarum* infestation in dwellings. Indoor Air. 14(3):196–199. [PubMed: 15104787]

Brasel TL, Douglas DR, Wilson SC, Straus DC. 2005 Detection of airborne *Stachybotrys chartarum* macrocyclic trichothecene mycotoxins on particulates smaller than conidia. Appl Environ Microbiol. 71(1):114–122. [PubMed: 15640178]

Buskirk AD, Green BJ, Lemons AR, Nayak AP, Goldsmith WT, Kashon ML, Anderson SE, Hettick JM, Templeton SP, Germolec DR et al. 2014 A murine inhalation model to characterize pulmonary exposure to dry *Aspergillus fumigatus* conidia. PLoS One. 9(10):e109855. [PubMed: 25340353]

Carey SA, Plopper CG, Hyde DM, Islam Z, Pestka JJ, Harkema JR. 2012 Satratoxin-G from the black mold *Stachybotrys chartarum* induces rhinitis and apoptosis of olfactory sensory neurons in the nasal airways of rhesus monkeys. Toxicol Pathol. 40(6):887–898. [PubMed: 22552393]

CDC. 1994 Acute pulmonary hemorrhage/hemosiderosis among infants---Cleveland, January 1993-November 1994. MMWR. 43:881–883. [PubMed: 7969010]

CDC. 1997 Update: pulmonary hemorrhage/hemosiderosis among infants---Cleveland, Ohio, 1993-1996. MMWR. 46:33–35. [PubMed: 9011781]

Cho S-H, Seo S-C, Schmechel D, Grinshpun SA, Reponen T. 2005 Aerodynamic characteristics and respiratory deposition of fungal fragments. Atmospheric Environment. 39(30):5454–5465.

Chung YJ, Copeland LB, Doerfler DL, Ward MD. 2010 The relative allergenicity of *Stachybotrys chartarum* compared to house dust mite extracts in a mouse model. Inhal Toxicol. 22(6):460–468. [PubMed: 20235799]

Croston TL, Nayak AP, Lemons AR, Goldsmith WT, Gu JK, Germolec DR, Beezhold DH, Green BJ. 2016 Influence of Aspergillus fumigatus conidia viability on murine pulmonary microRNA and mRNA expression following subchronic inhalation exposure. Clin Exp Allergy. 46(10):1315–1327. [PubMed: 27473664]

Etzel RA, Montana E, Sorenson WG, Kullman GJ, Allan TM, Dearborn DG, Olson DR, Jarvis BB, Miller JD. 1998 Acute pulmonary hemorrhage in infants associated with exposure to *Stachybotrys atra* and other fungi. Arch Pediatr Adolesc Med. 152(8):757–762. [PubMed: 9701134]

Górny RL, Reponen T, Willeke K, Schmechel D, Robine E, Boissier M, Grinshpun SA. 2002 Fungal fragments as indoor air biocontaminants. Applied and Environmental Microbiology. 68(7):3522–3531. [PubMed: 12089037]

Hodgson MJ, Morey P, Leung WY, Morrow L, Miller D, Jarvis BB, Robbins H, Halsey JF, Storey E. 1998 Building-associated pulmonary disease from exposure to *Stachybotrys chartarum* and *Aspergillus versicolor*. J Occup Environ Med. 40(3):241–249. [PubMed: 9531095]

Islam Z, Harkema JR, Pestka JJ. 2006 Satratoxin G from the black mold *Stachybotrys chartarum* evokes olfactory sensory neuron loss and inflammation in the murine nose and brain. Environ Health Perspect. 114(7):1099–1107. [PubMed: 16835065]

Jarvis BB, Sorenson WG, Hintikka EL, Nikulin M, Zhou Y, Jiang J, Wang S, Hinkley S, Etzel RA, Dearborn D. 1998 Study of toxin production by isolates of *Stachybotrys chartarum* and *Memnoniella echinata* isolated during a study of pulmonary hemosiderosis in infants. Appl Environ Microbiol. 64(10):3620–3625. [PubMed: 9758776]

Johanning E, Biagini R, Hull D, Morey P, Jarvis B, Landsbergis P. 1996 Health and immunology study following exposure to toxigenic fungi (*Stachybotrys chartarum*) in a water-damaged office environment. Int Arch Occup Environ Health. 68(4):207–218. [PubMed: 8738349]

Korpi A, Kasanen JP, Raunio P, Kosma VM, Virtanen T, Pasanen AL. 2002 Effects of aerosols from nontoxic *Stachybotrys chartarum* on murine airways. Inhal Toxicol. 14(5):521–540. [PubMed: 12028806]

Lemons AR, Hogan MB, Gault RA, Holland K, Sobek E, Olsen-Wilson KA, Park Y, Park JH, Gu JK, Kashon ML et al. 2017 Microbial rRNA sequencing analysis of evaporative cooler indoor environments located in the Great Basin Desert region of the United States. Environ Sci Process Impacts.

Lichtenstein JH, Molina RM, Donaghey TC, Amuzie CJ, Pestka JJ, Coull BA, Brain JD. 2010 Pulmonary responses to *Stachybotrys chartarum* and its toxins: mouse strain affects clearance and macrophage cytotoxicity. Toxicol Sci. 116(1):113–121. [PubMed: 20385656]

Madsen AM, Larsen ST, Koponen IK, Kling KI, Barooni A, Karottki DG, Tendal K, Wolkoff P. 2016 Generation and characterization of indoor fungal aerosols for inhalation studies. Appl Environ Microbiol. 82(8):2479–2493. [PubMed: 26921421]

Mensah-Attipoe J, Saari S, Veijalainen AM, Pasanen P, Keskinen J, Leskinen JTT, Reponen T. 2016 Release and characteristics of fungal fragments in various conditions. Sci Total Environ. 547:234–243. [PubMed: 26789361]

Montana E, Etzel RA, Allan T, Horgan TE, Dearborn DG. 1997 Environmental risk factors associated with pediatric idiopathic pulmonary hemorrhage and hemosiderosis in a Cleveland community. Pediatrics. 99(1):E5.

Nayak AP, Croston TL, Lemons AR, Goldsmith WT, Marshall NB, Kashon ML, Germolec DR, Beezhold DH, Green BJ. 2018 Aspergillus fumigatus viability drives allergic responses to inhaled conidia. Ann Allergy Asthma Immunol.

Nikulin M, Reijula K, Jarvis BB, Hintikka EL. 1996 Experimental lung mycotoxicosis in mice induced by *Stachybotrys atra*. Int J Exp Pathol. 77(5):213–218. [PubMed: 8977373]

Ochiai E, Kamei K, Watanabe A, Nagayoshi M, Tada Y, Nagaoka T, Sato K, Sato A, Shibuya K. 2008 Inhalation of *Stachybotrys chartarum* causes pulmonary arterial hypertension in mice. International Journal of Experimental Pathology. 89(3):201–208. [PubMed: 18460072]

Pestka JJ, Yike I, Dearborn DG, Ward MD, Harkema JR. 2008 *Stachybotrys chartarum*, trichothecene mycotoxins, and damp building-related illness: new insights into a public health enigma. Toxicol Sci. 104(1):4–26. [PubMed: 18007011]

Rand TG, Mahoney M, White K, Oulton M. 2002 Microanatomical changes in alveolar type II cells in juvenile mice intratracheally exposed to *Stachybotrys chartarum* spores and toxin. Toxicol Sci. 65(2):239–245. [PubMed: 11812928]

Rao CY, Brain JD, Burge HA. 2000 Reduction of pulmonary toxicity of *Stachybotrys chartarum* spores by methanol extraction of mycotoxins. Appl Environ Microbiol. 66(7):2817–2821. [PubMed: 10877773]

Rao CY, Burge HA, Brain JD. 2000 The time course of responses to intratracheally instilled toxic *Stachybotrys chartarum* spores in rats. Mycopathologia. 149(1):27–34. [PubMed: 11227851]

Reponen T 1995 Aerodynamic diameters and respiratory deposition estimates of viable fungal particles in mold problem dwellings. Aerosol Science and Technology. 22(1):11–23.

Reponen T, Seo SC, Grimsley F, Lee T, Crawford C, Grinshpun SA. 2007 Fungal fragments in moldy houses: a field study in homes in New Orleans and southern Ohio. Atmos Environ (1994). 41(37): 8140–8149. [PubMed: 19050738]

Rittenour WR, Ciaccio CE, Barnes CS, Kashon ML, Lemons AR, Beezhold DH, Green BJ. 2014 Internal transcribed spacer rRNA gene sequencing analysis of fungal diversity in Kansas City indoor environments. Environ Sci Process Impacts. 16(1):33–43. [PubMed: 24258337]

Saito R, Park JH, LeBouf R, Green BJ, Park Y. 2016 Measurement of macrocyclic trichothecene in floor dust of water-damaged buildings using gas chromatography/tandem mass spectrometry-dust matrix effects. J Occup Environ Hyg. 13(6):442–450. [PubMed: 26853932]

Seo S, Choung JT, Chen BT, Lindsley WG, Kim KY. 2014 The level of submicron fungal fragments in homes with asthmatic children. Environ Res. 131:71–76. [PubMed: 24657943]

Sorenson WG, Frazer DG, Jarvis BB, Simpson J, Robinson VA. 1987 Trichothecene mycotoxins in aerosolized conidia of *Stachybotrys atra*. Appl Environ Microbiol. 53(6):1370–1375. [PubMed: 3496850]

Templeton SP, Buskirk AD, Law B, Green BJ, Beezhold DH. 2011 Role of germination in murine airway CD8+ T-cell responses to *Aspergillus conidia*. PLoS One. 6(4):e18777. [PubMed: 21533200]

Yike I, Dearborn DG. 2004 Pulmonary effects of *Stachybotrys chartarum* in animal studies. Adv Appl Microbiol. 55:241–273. [PubMed: 15350797]

Yike I, Rand TG, Dearborn DG. 2005 Acute inflammatory responses to *Stachybotrys chartarum* in the lungs of infant rats: time course and possible mechanisms. Toxicol Sci. 84(2):408–417. [PubMed: 15647601]

Yike I, Vesper S, Tomashefski JF Jr., Dearborn DG. 2003 Germination, viability and clearance of *Stachybotrys chartarum* in the lungs of infant rats. Mycopathologia. 156(2):67–75. [PubMed: 12733626]

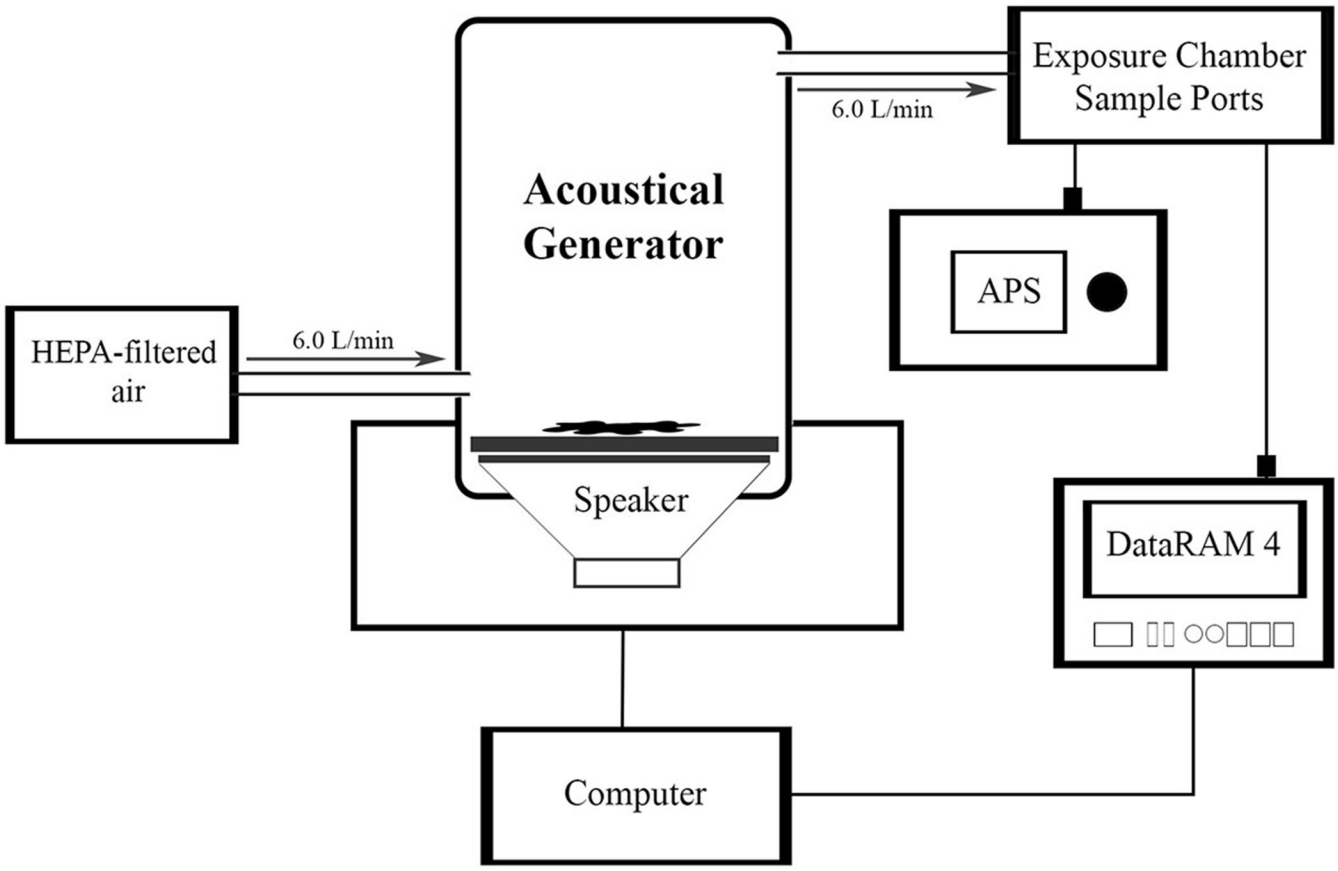

Figure 1.

An illustration depicting the acoustical generation system (AGS) used to aerosolize *S. chartarum* spores. Conidia-laden rice grains are placed on a rubber membrane within the generator where acoustical energy is used to aerosolize the *S. chartarum* spores. Spores can then be delivered to an exposure chamber where real-time particle size and concentration data are collected using the aerodynamic particle sizer (APS) and DataRAM 4.

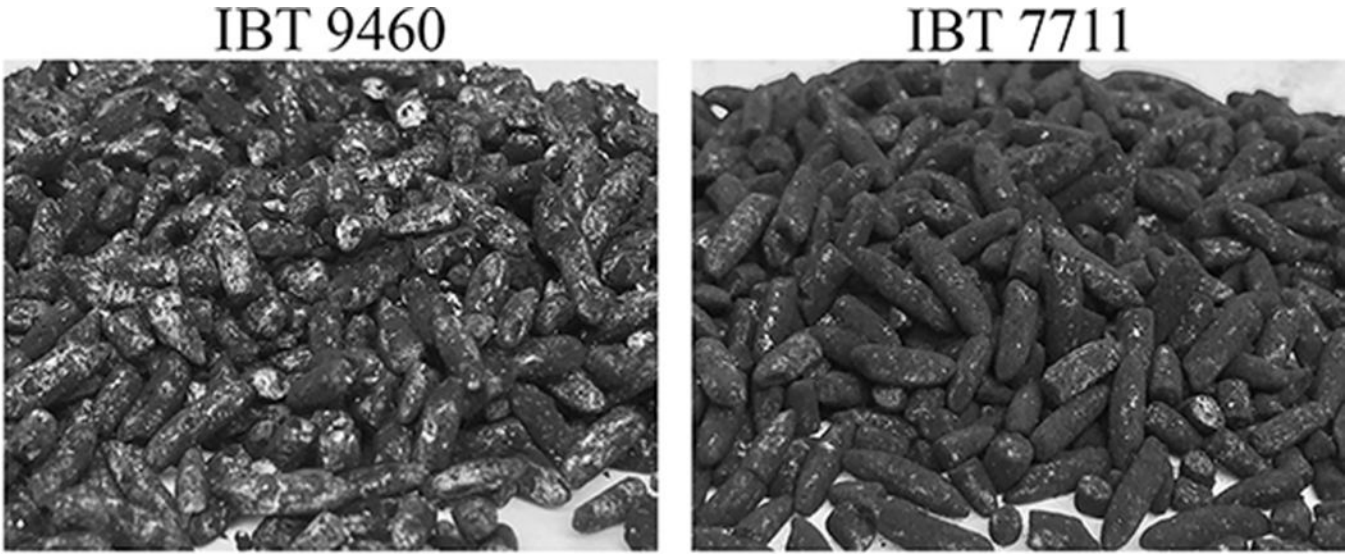

Figure 2.
Images presenting the growth of viable *S. chartarum* IBT 9460 and IBT 7711 on grains of white rice. Individual rice grains were almost entirely covered in sporulation *S. chartarum*.

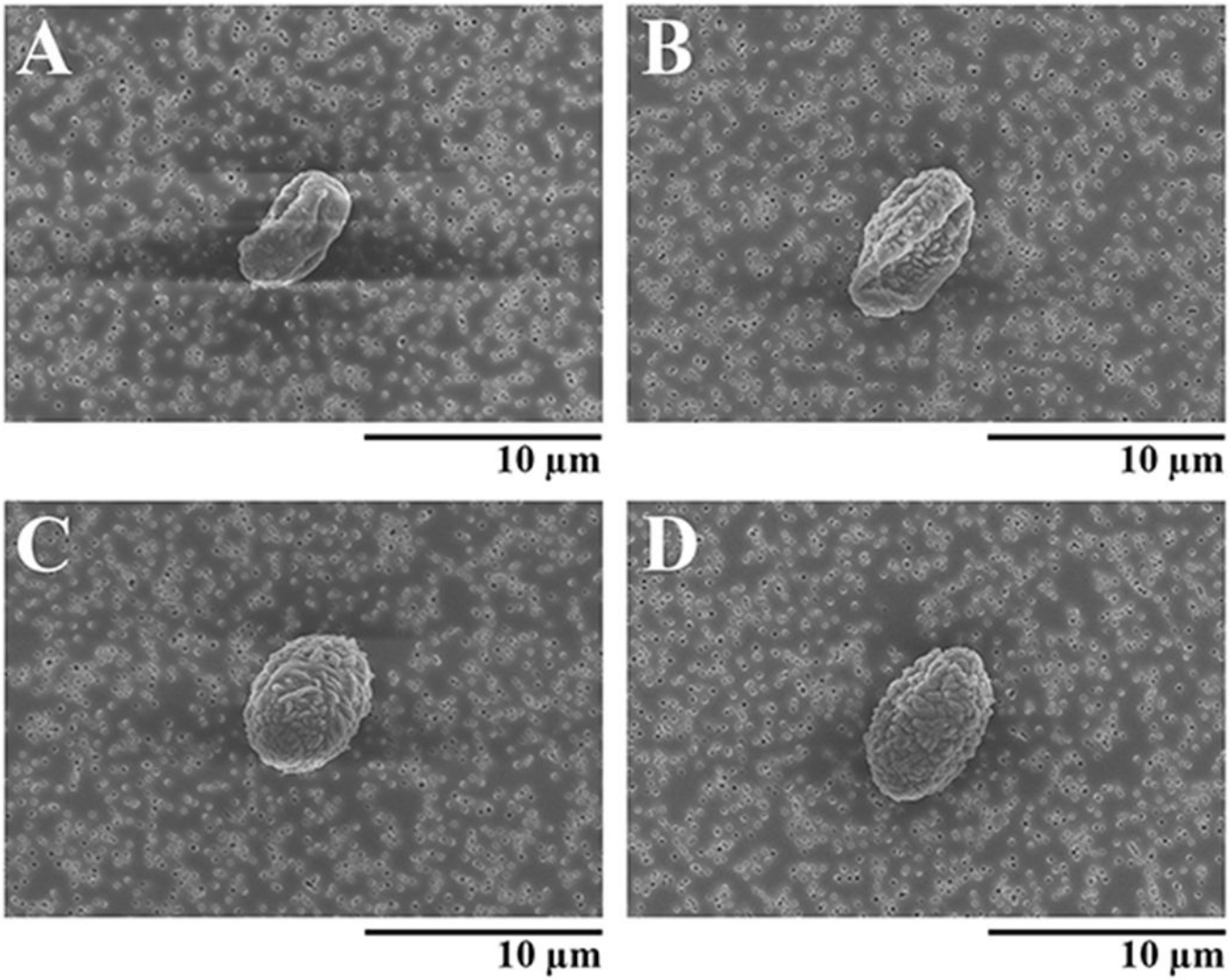

Figure 3.

Representative field emission scanning electron microscopy images of viable and heat-inactivated *S. chartarum* conidia derived from strains IBT 9460 and IBT 7711 illustrating no difference in conidia morphology following heat inactivation. (A) IBT 9460 viable conidia, (B) IBT 9460 heat-inactivated conidia, (C) IBT 7711 viable conidia, (D) IBT 7711 heat-inactivated conidia. Magnification, ×5000.

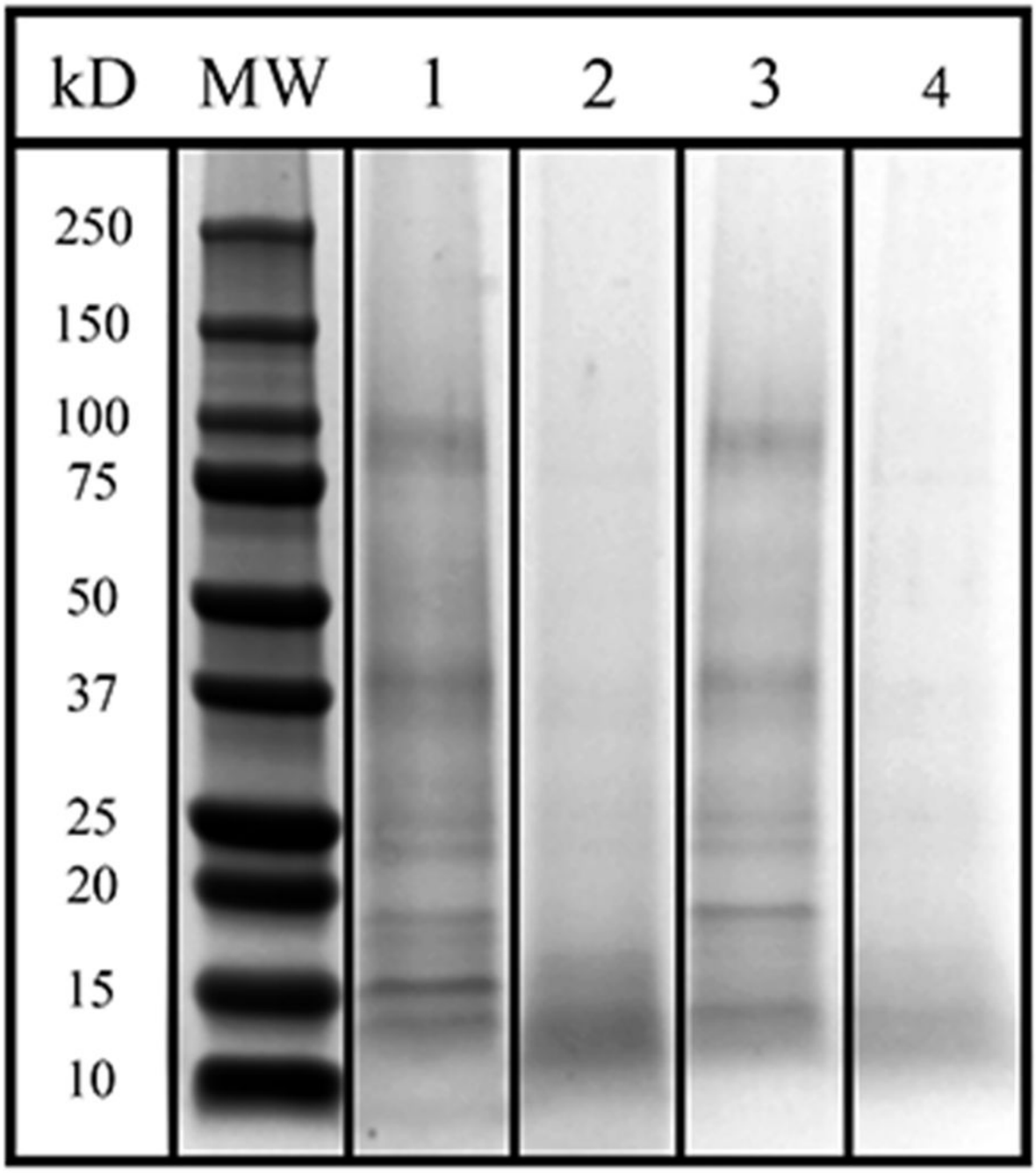

Figure 4.

Polyacrylamide gel electrophoresis analysis of *S. chartarum* conidia extracts prior to and after heat-inactivation. MW- molecular weight marker; Lane 1- IBT 9460 viable conidia extract; Lane 2- IBT 9460 heat-inactivated conidia extract; Lane 3- IBT 7711 viable conidia extract; Lane 4- IBT 7711 heat-inactivated conidia extract.

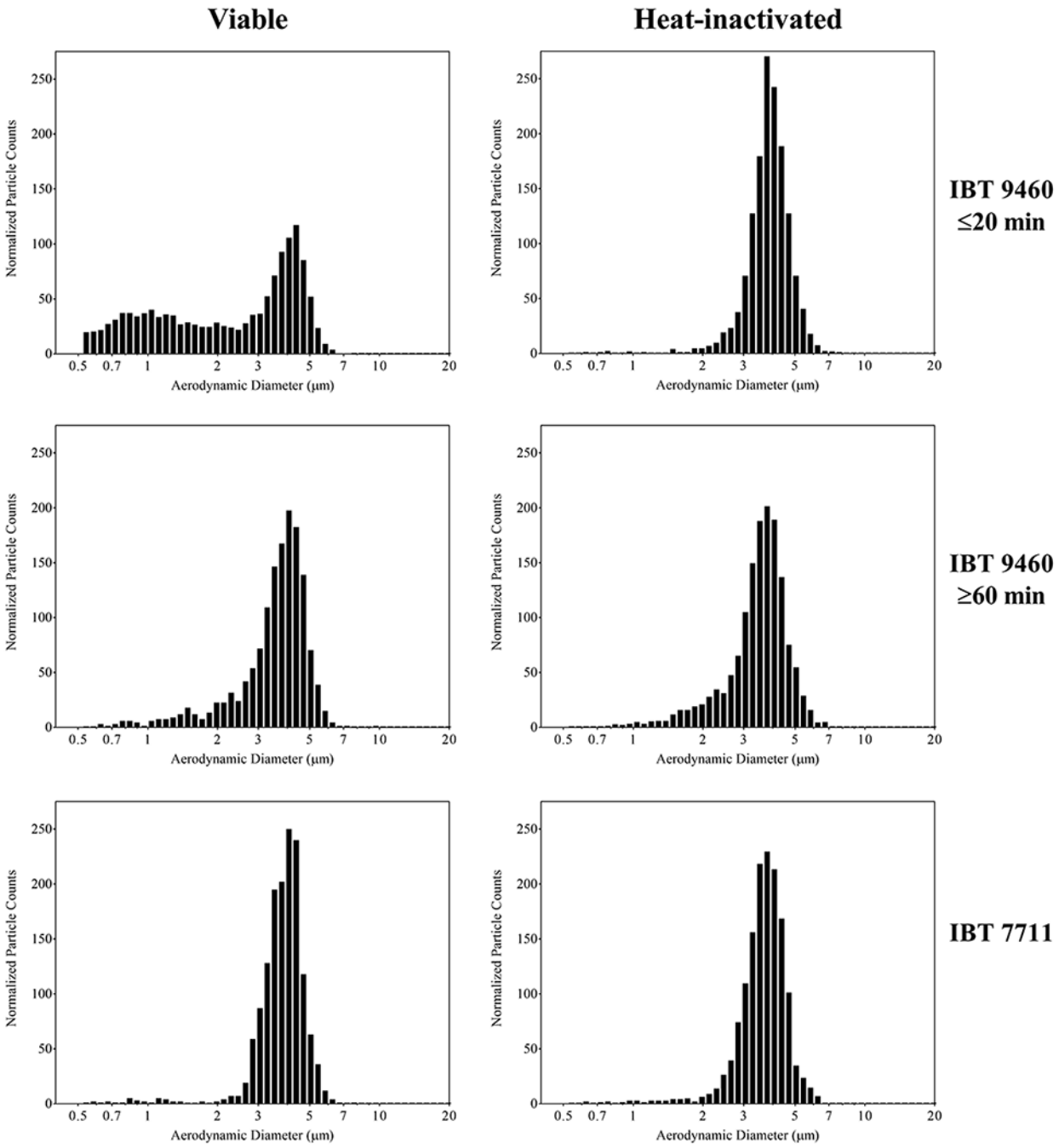

Figure 5.

Aerodynamic particle size distributions following aerosolization of viable and heat-inactivated *S. chartarum* conidia. The top 2 panels show the viable and heat-inactivated IBT 9460 aerosols captured during the early (≤20 min) and late (≥60 min) stages of aerosolization. The bottom panel shows the aerodynamic particle size distributions following aerosolization of *S. chartarum* IBT 7711 conidia, which remained constant throughout the course of the aerosolization. The graphs shown here are representative of the size

distributions observed over multiple aerosolization experiments and have been normalized based on the particle count concentration observed within the chamber for comparison.

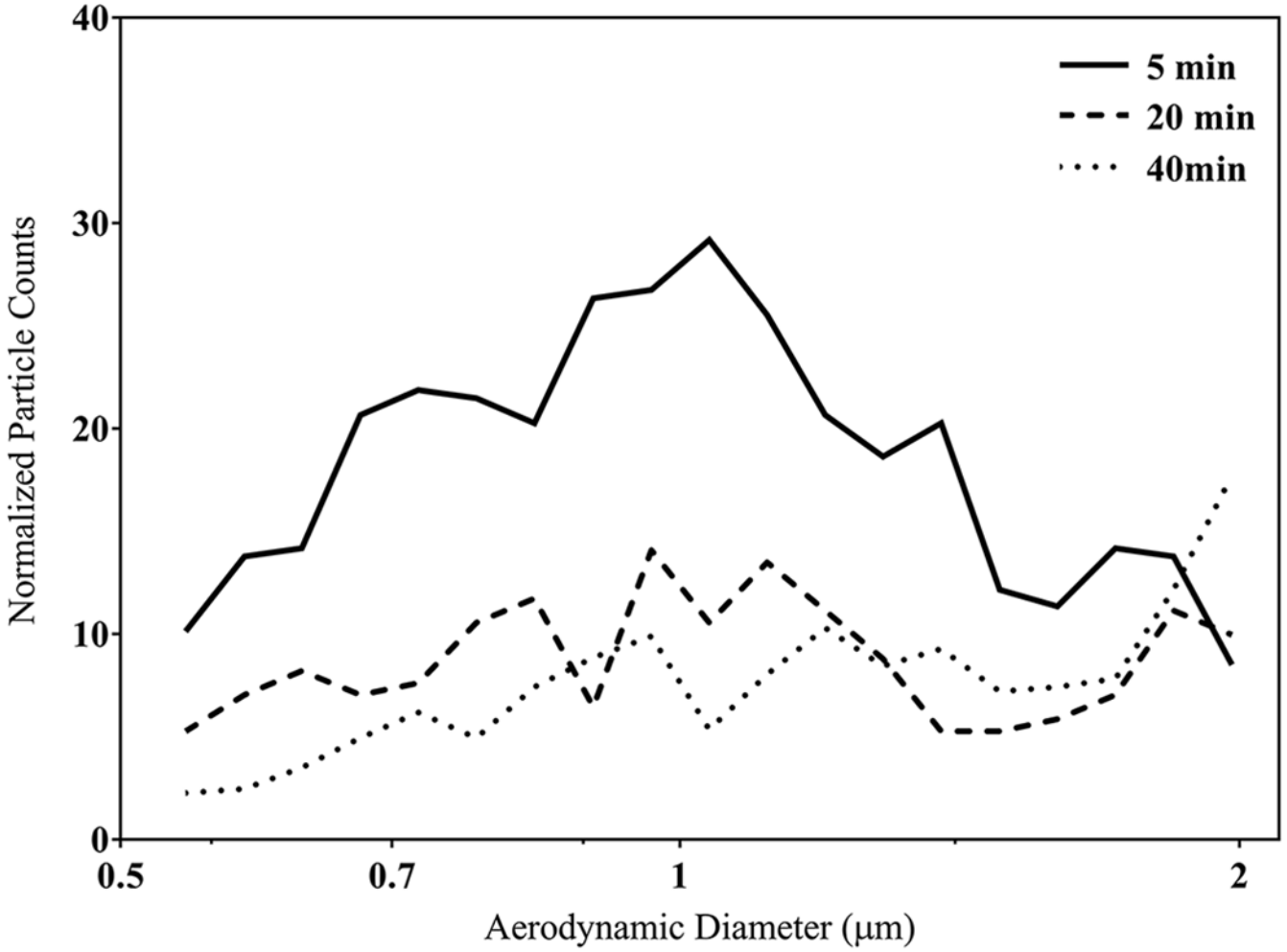

Figure 6.

The aerodynamic particle size distributions of the smaller fragments (0.5-2 μm) derived from viable *S. chartarum* IBT 9460 after 5 (solid line), 20 (dashed line) and 40 (dotted line) minutes of aerosolization. The size distributions at each time point have been normalized based on the particle count concentration observed within the chamber for comparison.

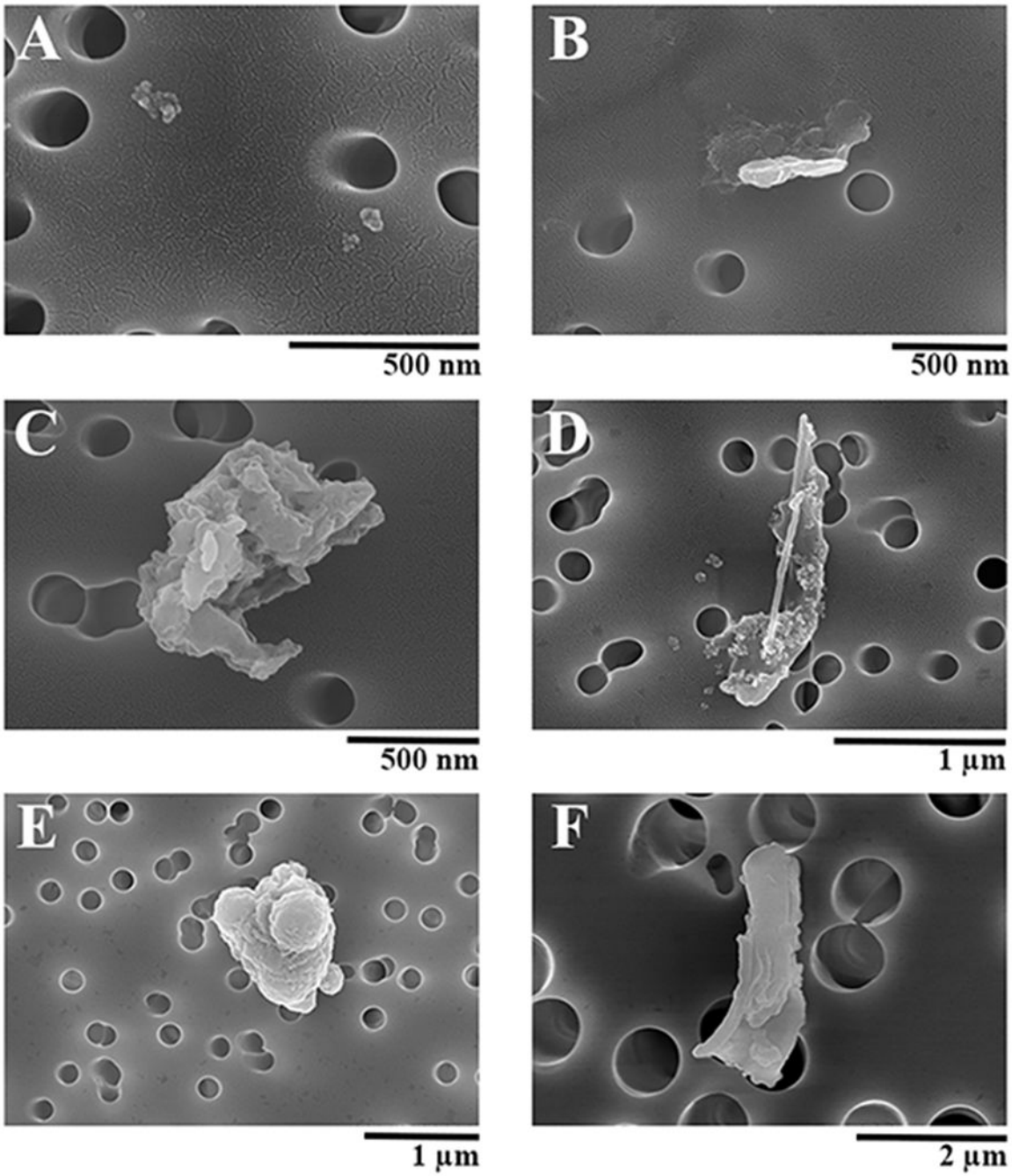

Figure 7.

Field emission scanning electron microscopy images of fragments derived from viable *S. chartarum* strain IBT 9460. Fragments appear to be derived from both conidia and hyphae and range in size from <0.5 µm to 2 µm. (A) Magnification, ×100,000; (B) Magnification, ×60,000; (C) Magnification, ×70,000; (D) Magnification, ×45,000; (E) Magnification, ×30,000; (F) Magnification, ×20,000.

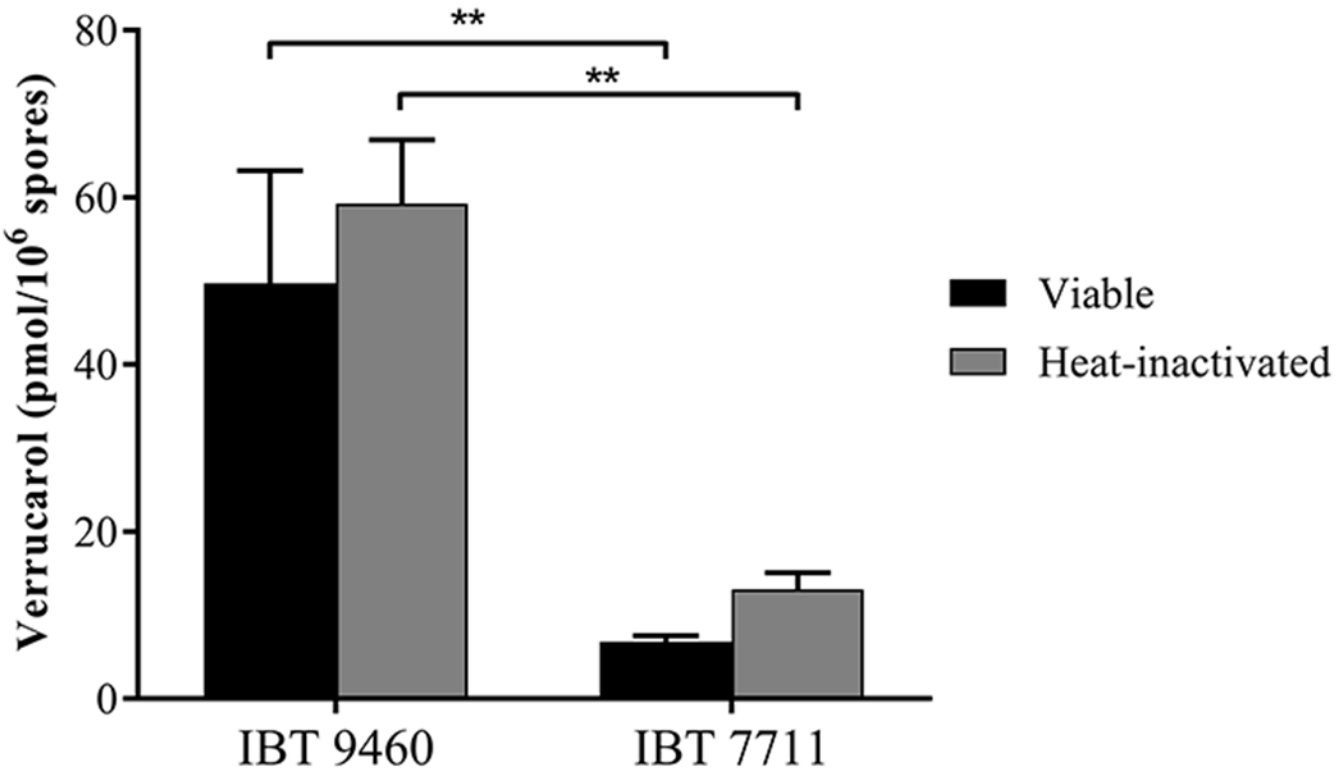

Figure 8.

UPLC/MSMS quantification of verrucarol present on polycarbonate filters sampled within the acoustical generator chamber following *S. chartarum* aerosolization. Verrucarol derived from aerosolized viable and heat-inactivated IBT 9460 and IBT 7711 strains. Based on the number of spores estimated to be deposited on the filter by real-time APS measurements, verrucarol (pmol) per 1 x 10^6 *S. chartarum* spores was calculated. Statistically significant differences were observed between strains ($p < 0.01$) but not as a result of heat-inactivation.

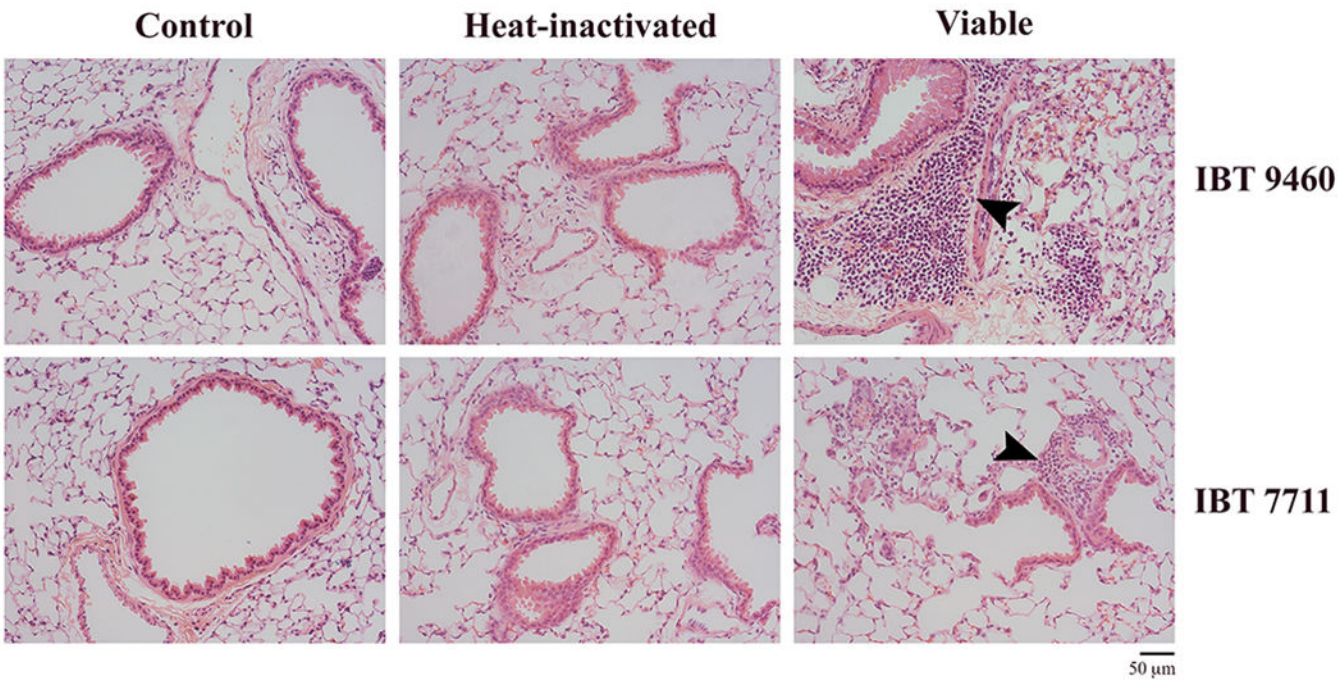

Figure 9.

Representative photomicrographs of murine lung sections following exposure to *S. chartarum* IBT 9460 (top panel) or IBT 7711 (bottom panel). Images shown represent air-only control (n=3), heat-inactivated (n=3/strain), or viable (n=3/strain) *S. chartarum* exposures. Airway inflammation (indicated by the black arrowheads) was observed following exposure to both viable strains of *S. chartarum*, but not following exposure to heat-inactivated *S. chartarum*. Images were captured using a 20X objective.

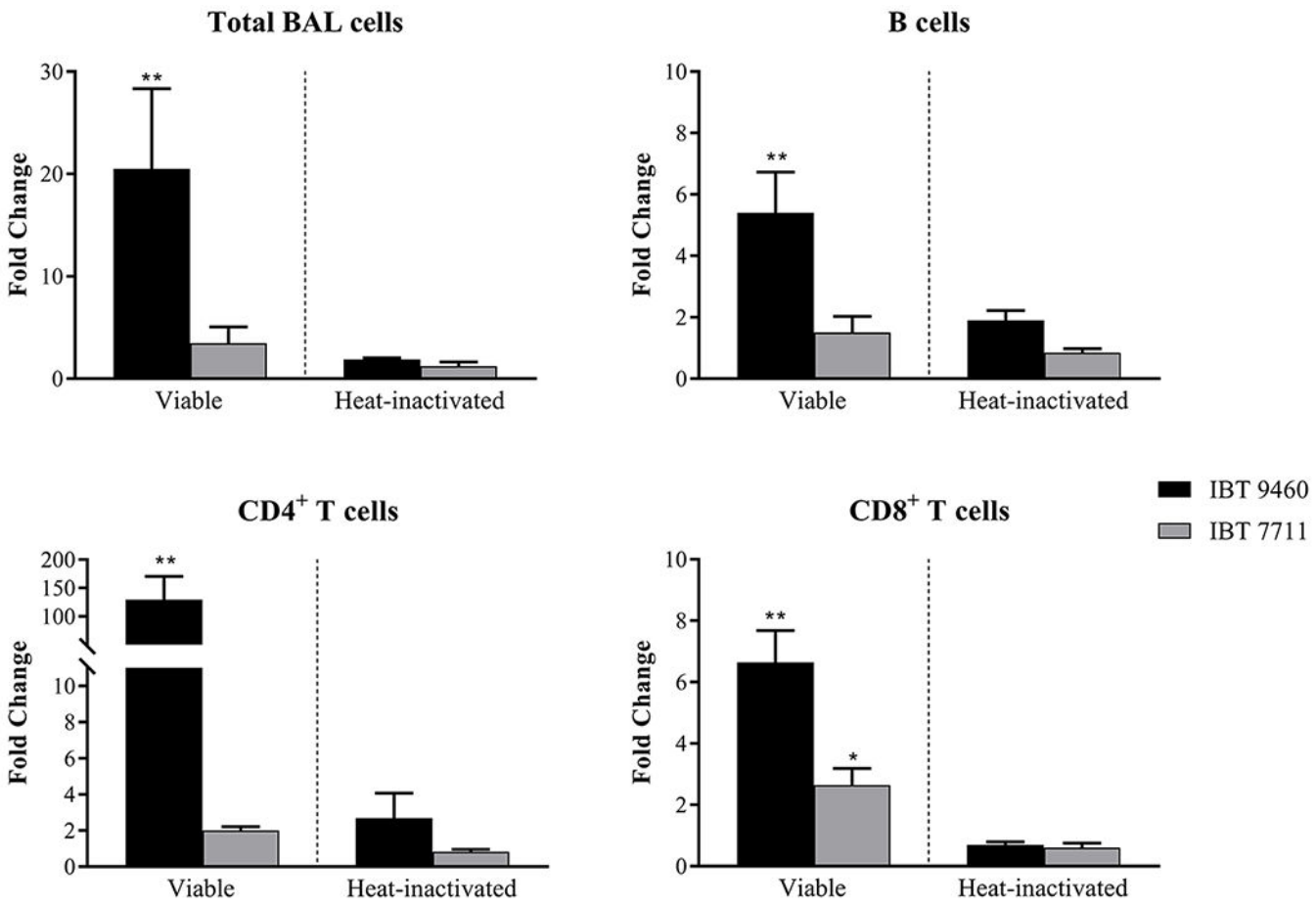

Figure 10.

Changes in bronchoalveolar lavage cell populations after exposure to *S. chartarum* IBT 9460 or IBT 7711. Graphs represent the fold change in cell number compared to air-only controls for total BAL cells, B cells, $CD4^+$ T cells and $CD8^+$ T cells as determined by flow-cytometry. Statistically significant increases in each cell population were observed following exposure to viable, but not heat inactivated *S. chartarum* IBT 9460 (** represents a $p < 0.01$). Increases, although not significant, were also seen following exposure to viable *S. chartarum* IBT 7711 (* represents $p = 0.05$).

Table 1.

Measurements within the AGS during murine exposures.[a]

Test Article	Temperature (°C)	Humidity (%)	Mass Concentration (mg/m^3)
***S. chartarum* IBT 9460**			
Viable	23.1 ± 0.8	47.3 ± 3.6	8.86 ± 1.76
Heat-inactivated	21.6 ± 0.8	47.4 ± 4.0	6.95 ± 1.10
***S. chartarum* IBT 7711**			
Viable	21.0 ± 0.7	46.6 ± 2.3	8.06 ± 1.47
Heat-inactivated	21.7 ± 0.5	33.4 ± 3.6	7.24 ± 1.98

[a]Measurements represent the average recorded over 8 animal exposures ± standard deviation.

Table 2.

Viability of *S. chartarum* conidia following prior to and following heat-inactivation.

Test Article[a]	Percentage Viable Spores
***S. chartarum* IBT 9460**	
Viable	53.50 ± 13.20
Heat-inactivated	0[b]
***S. chartarum* IBT 7711**	
Viable	60.75 ± 7.63
Heat-inactivated	0[b]

[a] n=4 test articles with 2 replicates per group. Values represent the average percentage of viable spores ± standard deviation.

[b] Heat inactivation resulted in 100% reduction in spore viability for both strains tested.

Table 3.

Proportion of fragments observed following aerosolization of *S. chartarum* conidia-laden rice cultures.[a]

Test Article	Percentage of Particles <2 μm (aerodynamic diameter)	Percentage of Particles >2 μm (aerodynamic diameter)
***S. chartarum* IBT 9460 (≤20 min)**		
Viable	50.58% ± 1.40%	49.42% ± 1.40%
Heat-inactivated	2.25% ± 0.35%	97.75% ± 0.35%
***S. chartarum* IBT 9460 (≥60 min)**		
Viable	10.86% ± 0.48%	89.14% ± 0.48%
Heat-inactivated	9.58% ± 0.18%	90.42% ± 0.18%
***S. chartarum* IBT 7711**[b]		
Viable	4.87% ± 1.43%	95.13% ± 1.43%
Heat-inactivated	4.11% ± 1.48%	95.89% ± 1.48%

[a]The proportions presented in the table are representative of the size distributions observed over multiple aerosolization experiments. Measurements for IBT 9460 (n=3) were obtained at each time interval (≤20 min and ≥60 min) while measurements for IBT 7711 (n=6) were obtained over the course of a 60 min aerosolization. Values represent the average percentage ± standard deviation.

[b]Time course measurements of *S. chartarum* IBT 7711 showed no difference in size distribution at varying time intervals.